Agronomy Research **19**(3), 1423–1435, 2021
https://doi.org/10.15159/AR.21.141

Comparison of spatial-temporal analysis modelling with purely spatial analysis modelling using temperature data obtained by remote sensing

L.M. dos Santos[1,*], G.A.S. Ferraz[1], H.J.P. Alves[2], J.D.P. Rodrigues[3], S. Camiciottoli[4], L. Conti[4] and G. Rossi[4]

[1]Federal University of Lavras, Department of Agricultural Engineering, University Campus, BR37.200-000 Lavras-MG, Brazil
[2]Institute of Applied Economic Research- IPEA, Rio de Janeiro, BR 20071-900 Rio de Janeiro, Brazil
[3]Geoprocessing Analyst, Bracell, Lençois Paulistas, BR17120-000 São Paulo, Brazil
[4]University of Firenze, Department of Agriculture, Food, Environment and Forestry, Via San Bonaventura, 13, Firenze, Italy
[*]Correspondence: luanna_mendess@yahoo.com.br

Received: March 25th, 2021; Accepted: May 20th, 2021; Published: October 5th, 2021

Abstract. Variations in climatic elements directly affect the productivity of agricultural activities. Temperature is one of the climatic elements that varies in space and time.Therefore, understanding spatial variations in temperature is essential for many activities. Given the above, the objective of this work was to compare the performance of the proposed spatiotemporal analysis model with that of purely spatial analysis using temperature data obtained by remote sensing. The experimental data were arranged in a grid with 403 spatial locations, with 22 samples collected in a 24-hour period. The statistical software R Core Team (2020) was used to perform the analysis. The packages used in the analyses were 'geoR', 'CompRandFld', 'scatterplot3d', and 'fields'. For making the maps, the software ArcGIS was used. The behavioural analysis of spatiotemporal dependence indicated, through the covariogram graph of the data, that there is a strong spatial dependence. For the cases of purely spatial analysis of phenomena, a separate spatial model for each time is justified because this type of model presents a smaller prediction error and requires simpler processing than the space-time model. It was possible to compare the space-time analysis with the purely spatial analysis using temperature data obtained by remote sensing images. The data modelled with the purely spatial analysis had, on average, lower error than those with the space-time model.

Key words: climatic elements, geostatistics, mathematical modelling.

INTRODUCTION

Agricultural activities are always susceptible to the variations in climatic elements and consequently to risks. Temperature is one of the climatic elements that varies in space and time, and this parameter participates in several physiological processes in

plants and animals. Thus, understanding this element is important and relevant for evaluating studies on crop adaptation and agricultural planning (Coelho et al., 1973; Medeiros et al., 2005). Temperature is also important for the indication of the sowing time, irrigation, determination of yield potential, credit, and agricultural insurance (Cargnelutti Filho et al., 2008).

According to Viana et al. (2019), the temperature has strong temporal dependence, causing the energy received by Earth to vary mainly due to the rotational (variation in the day) and translational (variation in the year) movements of the Earth, in addition to having spatial variations, depending, for example, on the movements of air masses and variations in the surface, such as soil cover, albedo, altitude, and humidity.

Understanding the spatiotemporal dependence of temperature is essential for many activities. However, meteorological data are usually acquired in an ad hoc and isolated manner through automatic weather stations (Hartkamp, 1999). According to Varejão-Silva (2006), although there are large air temperature data series available for some locations in certain regions, there may be no records for the exact location one is interested in studying. In addition, according to Medeiros et al. (2015), there are a small number of weather stations, making the density of available temperature data low and making it difficult to characterize the thermal field. These situations are very common in practice and promote the development of techniques that seek to estimate the temperature in locations for which there are no data (Medeiros et al., 2015).

Thus, it is possible to obtain temperature data from satellite images. The series of geostationary satellites Meteosat Second Generation (MSG), in orbit since 2002, uses the spinning enhanced visible and infrared imager (SEVIRI) sensor and produces images in 12 spectral channels with a spatial resolution of 3 km at nadir, a temporal resolution of 15 minutes, and a radiometric resolution of 10 bits (Schmetz et al., 2002). MSG is useful for data acquisition and subsequent spatialization with good temporal resolution. However, satellite image data must be subjected to radiometric corrections to reduce the influence of the atmosphere (Geiger et al., 2008). Another factor that interferes with image acquisition is the weather conditions. On cloudy days, for example, the passage of solar energy is blocked by clouds, with the consequent loss of surface data (Honkavaara et al., 2013).

Given the loss of information, the spatialization of this variable can be performed using interpolation techniques in which values are estimated in unsampled locations, and maps can be created with continuous data in space; these procedures are part of geostatistics.

Currently, geostatistical methods facilitate the interpretation of data randomness, in addition to being an efficient tool for spatializing climatic elements (Pessanha et al., 2020), predicting noise from agricultural machinery (Santos et al., 2020), and predicting data within animal facilities (Curi et al., 2014; Cemek et al., 2016, Ferraz et al., 2016; Damasceno et al., 2019; Ferraz et al., 2019; Oliveira et al., 2019), among other applications in which the maps generated by this method facilitate data interpretation. However, these studies, although working with spatiotemporal data, performed purely spatial analyses and did not concomitantly explore the interaction between the spatial and temporal components.

The application of spatiotemporal geostatistics, through covariance structure modelling, is one of the procedures for spatiotemporal data analysis that takes into account the interactions between the spatial and temporal components and allows

interpolations in time and space (Viana et al., 2019). This procedure was proposed by Gneiting (2002) and allows the simultaneous performance of spatial and temporal analyses.

Thus, the objective of this study was to compare the performance of the proposed spatiotemporal analysis with that of purely spatial analysis using temperature data obtained by remote sensing.

MATERIALS AND METHODS

Data Acquisition

The study area (Fig. 1) is located in the municipality of Lavras, in the state of Minas Gerais (MG), in the southeastern region of Brazil between latitude 21° 14' 45' south and longitude 45° 00' W of Greenwich, with a maximum altitude of 918 m above sea level (ASL). The municipality of Lavras is in an ecotone of the Cerrado and Atlantic Forest domains, where remnants of seasonal semideciduous forest, grassland, montane savanna, and cerrado (Brazilian savanna) are found (Souza et al., 2003; Dalanesi et al., 2004; Pereira et al., 2010). The climate of the region, according to the Koppen classification, is of the Monsoon-influenced humid subtropical climate (Cwa) type, characterized by a dry season in the winter and a rainy season in the summer. The average annual precipitation is 1,460 mm, and the average annual temperature is 20.4 °C, with a minimum of 17.1 °C in July and a maximum of 22.8 °C in February (Dantas et al., 2007).

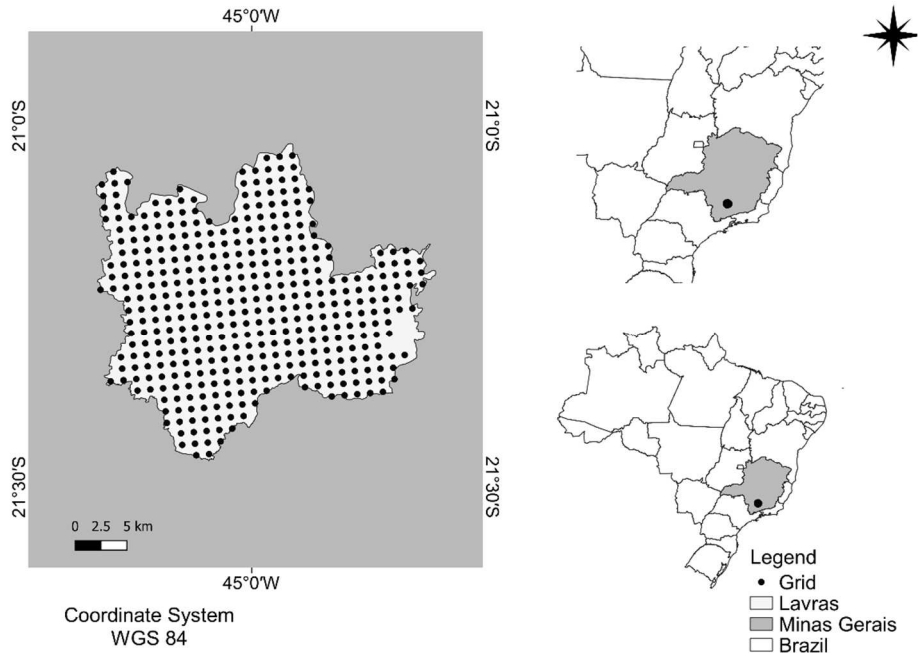

Figure 1. Location of the municipality of Lavras, MG.

Data were obtained with images from the MSG series of geostationary satellites of the European Organization for the Exploitation of Meteorological Satellites (EUMETSAT). These satellites have instruments such as the geostationary earth radiation budget (GERB) radiometer, communication instruments such as geostationary search and rescue (GEOS&R), the data collection system (DCS) data storage platform, and the SEVIRI sensor.

The SEVIRI sensor is equipped with 12 spectral channels, ranging from visible wavelengths to far-infrared wavelengths, including absorption bands of water vapor, ozone (O_3), and carbon dioxide (CO_2), with a spatial resolution between 1 km and 3 km at nadir (Fensholt et al., 2006). MSG stands out as the first series of geostationary satellites in the world with red and near infrared (NIR) bands, which are very useful for monitoring the Earth's surface at high temporal resolution (Schmetz et al., 2002).

With this temporal resolution, meteorological images can be obtained every 15 minutes in nominal mode or every 5 minutes in rapid scan mode. Thus, the values obtained every 15 minutes by MSG can be acquired 96 times a day. However, in this study, we used 22 observations of mean temperature values collected during the 1 July 2013, thus obtaining the temperature from time 1 to time 22, in which time 1 corresponded to 00 h and time 22 corresponded to 5 h 15 AM of the chosen day. These parameters were randomly selected to test the models under study.

The images were corrected following the methodology proposed by Geiger et al. (2008). The correction of atmospheric effects is important due to the dynamics of atmospheric components (aerosols, gases and clouds). For this, the SMAC (Simplified Method for Atmospheric Correction) technique is used, which demands less time. The data were arranged in a grid with 403 spatial locations spaced 1 km apart. A total of 403 locations were used to cover the entire study region (Fig. 1).

Space-time random fields

Let Z (s,t) be a random variable measured at position s in Rd, and at time t in R, Rd is the space, R is the time, and Rd x R is the domain of the random field defined in space-time. In this sense, a space-time random field is defined as Z (s,t), where s is in Rd and t is in R. In this article, d = 2 is considered such as in the study by Rodrigues et al. (2019). However, note that d can be any positive integer.

Kriging

The linear kriging predictor is defined as Z (s0,t)= $\mu_z + \sigma'\Sigma^{-1}(Z - \mu_z)$. The case where μ is constant but unknown denotes ordinary kriging. This estimator must meet the following criteria:

$[Z(s_0,t_0)-\widehat{Z}(s_0,t_0)]=0$; that is, it should be unbiased;

Var $[Z(s_0,t_0)-\widehat{Z}(s_0,t_0)]$is minimal.

Generally, sampling is performed with a set of points distributed sparsely throughout the region. The objective is to continuously describe the process throughout the region. However, for the case of the prediction of space-time random fields, obtaining theoretical models of semivariograms can be very complicated. A simpler method is to consider theoretical models of the stationary covariance functions that are valid.

Covariance functions

In geostatistics, for each sampled location spatially and temporally located, there is only one realization, and the number of observations is always finite. This condition usually makes it impossible to infer the probability distribution of the location. Therefore, some hypotheses are necessary, including one commonly called the hypothesis of stationarity. Assuming this second-order hypothesis, the covariance is a tool that can be used for the autocorrelation between pairs of measured values separated by a distance h. According to Sherman (2011), a moments estimator for the covariance is defined according to equation (1):

$$\widehat{C}(h,u)=\frac{1}{N(h,u)}\sum_{N(h,u)}\{[Z(s_1,t_1)-\mu][Z(s_2,t_2)-\mu]\}^2 \quad (1)$$

where N(h,u) is the number of points that are within the distance h in each time lag u and μ is the mean of the random field.

Gneiting's model (2002)

Gneiting (2002) proposes the direct construction of classes of nonseparable stationary space-time covariance functions in the space-time domain. Consider two conveniently chosen functions $\varphi(r), r \geq 0$ and ψ(r). The first is a completely monotone function, and the second is a positive function with a completely monotone derivative. These definitions can be seen in Gneiting (2002), which presents the following model given by Eq. (2):

$$C(h,u)=c_0+\frac{\sigma^2}{(a|u|^{2\alpha}+1)^{\delta+\beta}}\exp\left(-c\frac{\|h\|^{2\gamma}}{(a|u|^{2\alpha}+1)^{\beta\gamma}}\right) \quad (2)$$

where ‖h‖ is the spatial distance, |u| is the time lag, σ^2 is the variability present in the random field, and $c_0 = \frac{\sigma^2_{h=0}}{a|u|^{\delta}}$ is the nugget effect that is defined as an uncontrollable sampling error. Eq. (2) is implemented in the 'CompRandfld' package available in the R software and is used in the data analysis, where a, c, and $\sigma^2 > 0$ and α,γ,β ∈(0,1]. Here, a and α are the scaling and smoothness parameters of the process in time; c and γ are the scale and smoothness parameters of the process in space. The parameter β measures the strength of the space-time interaction.

Software used

The free statistical software R version 3.5.0 (Team, 2020) was used to perform the geostatistical analyses. The packages used in the analyses were 'geoR' (Ribeiro Júnior & Diggle 2020), 'CompRandFld' (Padoan & Bevilacqua, 2020), 'scatterplot3d' (Ligges et al., 2020), and 'fields' (Nychka et al., 2020); these packages are essential for working with spatiotemporal geostatistics. The standard format of a spatiotemporal database has coordinates (x, y) of the locations, with values of the attribute (z), in this case, the average temperature in addition to the times/dates of the measurements.

The calculated values of kriging prediction and variance were exported in text format (.txt) to ArcGIS to prepare the maps. The universal transverse Mercator (UTM) coordinate system, datum WGS 84, zone 23 south, was used with the intention of adaptation to the field data.

RESULTS AND DISCUSSION

Spatiotemporal behaviour

The existence of a spatiotemporal relationship in the data is the key point for the use of the space-time covariance function models proposed, as observed in Fig. 2.

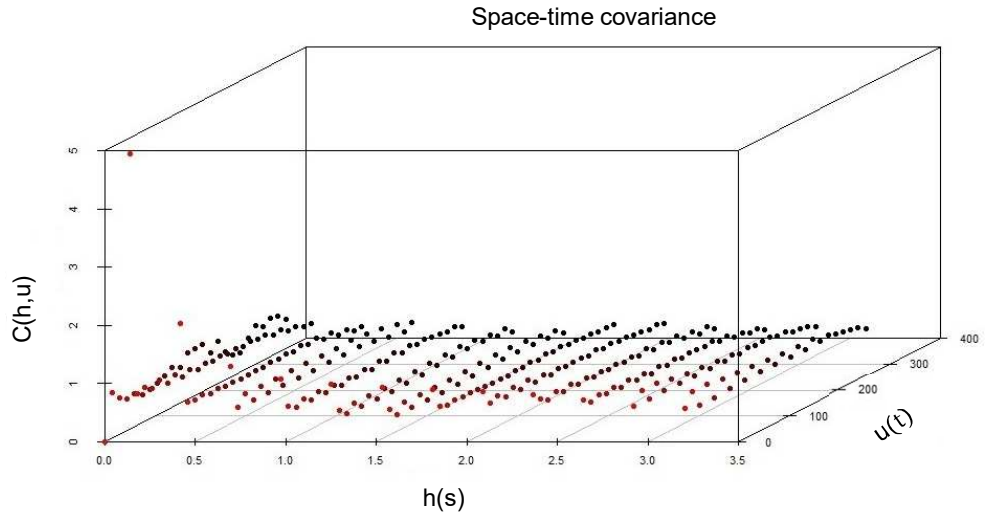

Figure 2. Sample covariogram.

Spatiotemporal analysis

The space-time covariance function model proposed by Gneiting (2002) is given by Eq. (3):

$$C(h,u)=1.728e^{-7}+\frac{2.002}{(2.082|u|^{7.084e-01}+1)^{1}}\exp\left(1.468\frac{0.008634\|h\|^{6.685e-01}}{(2.082|u|^{7.084e-01}+1)^{1}}\right) \qquad (3)$$

Table 1 shows the estimated parameters for the covariance model according to Eq. (3):

Table 1. Estimated parameters of Gneiting's model (2002)

C_0	σ^2	a	α	c	γ	β
0.0000001728	2.002	2.082	1	1.468	1	1

C_0 is the nugget effect; σ^2 is the random field variance, a is the scale parameter in time; α is the smoothness parameter in time; c is the scale parameter in space; γ is the smoothness parameter in space, and β is the parameter that measures the strength of the space-time interaction.

In the analysis of the behaviour of the spatiotemporal dependence between the data, a covariogram plot is a useful tool. Fig. 3 shows the spatiotemporal covariogram fitted to the data. Strong spatial dependence is perceived because $\beta = 1$, and this parameter measures the strength of the space-time interaction.

With classical statistics, the interaction between space and time cannot be obtained; i.e., the variability in the space and time dimensions cannot be collectively captured (Bicalho, 2008). With the spatiotemporal model, the covariogram shows that the spatiotemporal dependence is short-range. This means that this dependence is strong, indicating that the influence between the points ceases to exist within short distances in

space and time in the study area; that is, when travelling 1.48 km in space and 34.7 hours in time, there is no longer a dependence.

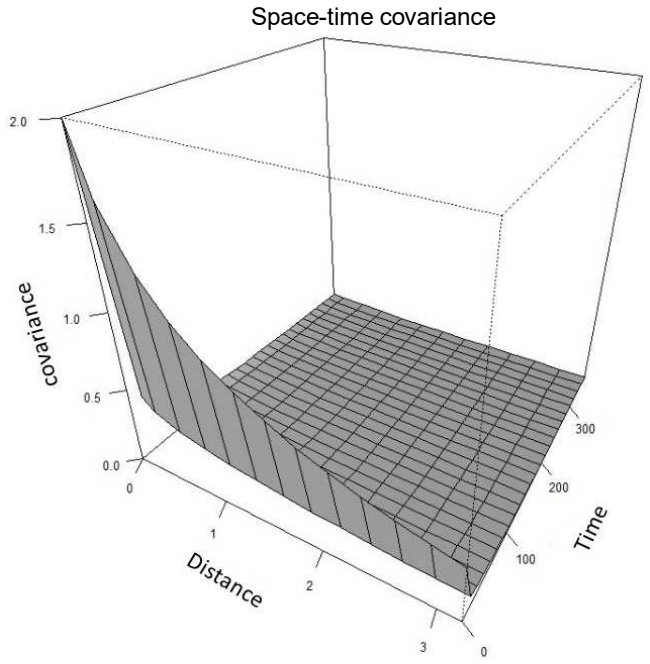

Figure 3. Spatiotemporal covariogram fitted to the data.

The ordinary kriging technique is a linear predictor that requires continuity in the study area to be applied, which assumes that there is a mean in the random field studied but that it is unknown. This provides the maps that generally serve as a visual information instrument to continuously investigate patterns of occurrence of some phenomena in the study area. The maps obtained over the period of the studied day show the temperature variation and the interaction that occurs between the phenomenon in space and time.

The maps show the daily evolution of the temperature of the city of Lavras, MG, over a day. Fig. 4 shows that the temperature ranged from a minimum of 9.5 °C to 18 °C because it considers a winter day, in which the temperature ranges from 11 °C to 25 °C. In addition, the analyses and maps were prepared with temperature data from 00:00 to 05:15 AM in the morning of the studied day. Thus, the resulting temperature is characterized as mild in this period. A temperature classification table was proposed in this study to help identify the thermal sensation at the study site (Table 2). This table classified temperature ranging from 0 °C to 7 °C as very cold; from 7 °C to 13 °C as cool; from 13 °C to 18 °C as mild; from 18 °C to 24 °C as pleasant; from 24 °C to 29 °C as warm; from 29 °C to 35 °C, as hot, and above 35 °C as scorching.

Table 2. Characterization of the mean hourly temperatures

	Temperature (°C)	Characterization
Classes	0 to 7	Very cold
	7 to 13	Cool
	13 to 18	Mild
	18 to 24	Pleasant
	24 to 29	Warm
	29 to 35	Hot
	> 35	Scorching

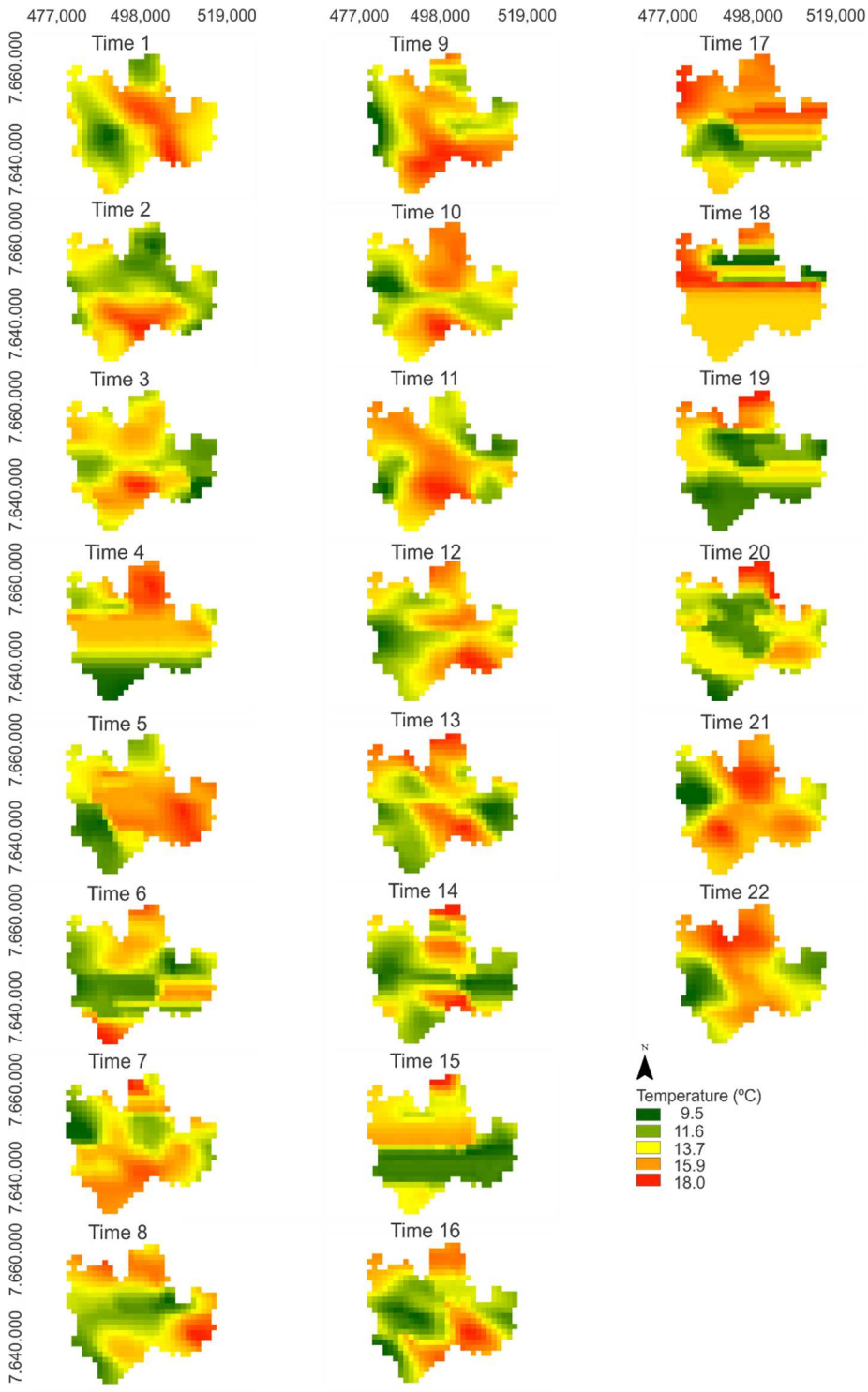

Figure 4. Interpolation maps of the mean air temperature using ordinary kriging from time 1 to time 22 for the studied day.

Fig. 4 shows that from time 1 (00 h) to time 3 (00 h 30), the temperature can be classified according to Table 2 as mild, as most of the area stayed between 13 °C and 18 °C. From time 4 (00 h 45) to time 22 (5 h 15 AM), the temperature can be classified according to Table 2 as cool, ranging from 7 °C to 13 °C, showing some transition regions with mild temperature.

The warmest zones, i.e., the red- and orange-coloured areas of the maps, especially at times 2, 3, and 18, were observed in the central region where the highest population density is found. The boundary regions are farm regions with greater vegetation, so the temperature in these areas were predominantly shaded green.

The maps presented in Fig. 4 may contain errors, and a way to assess whether the proposed model fits the data well is to evaluate its residuals (Fig. 5). They should be well-behaved with minimum values. The residual is defined as $E\left[\widehat{Z_{(s,t)}} - Z_{(s,t)}\right]$, where $\widehat{Z_{(s,t)}}$ is the value estimated by the model and $Z_{(s,t)}$ is the real value.

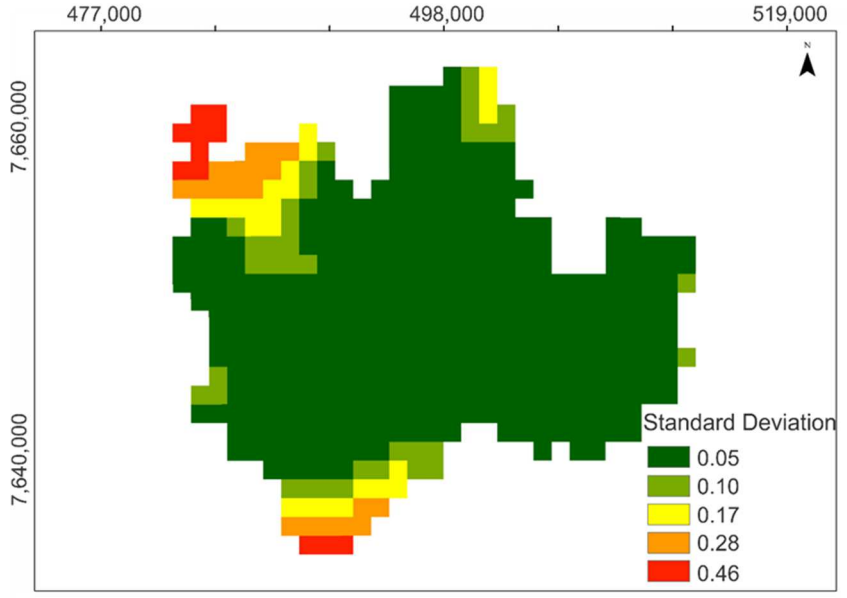

Figure 5. Residuals map.

When the error maps are presented, they are consistent, which indicates little variation in errors between the measured times. This is a great result. The intention is not to determine if this is the best model for these data but to compare the performance of this model with another model and to determine which is the best option for data analysis: stationary space-time covariance functions or a purely spatial model, separated by each time.

Purely spatial analysis

In this study, we did not seek to produce kriging maps but rather a descriptive analysis of the standard deviations of the prediction errors. It is reasonable to assume that the model with the smallest prediction error is the best choice. The purely spatial dependence model with best fit to the data was the exponential model, taking into

account the criterion of greater range, the nugget effect, and the spatial contribution. These results were used in the construction of Table 3. This choice is usually made 'by feeling' because there are no statistical tests that indicates which model should be fitted. The respective parameters were estimated using the least squares method.

Table 3. Comparison between the two models, where the descriptive measures of the minimum, mean, and maximum were evaluated for the standard deviations of the prediction errors

Time	Space-time			Purely Spatial		
	Minimum	Mean	Maximum	Minimum	Mean	Maximum
Time 01	0.0381	0.0488	0.0828	0.0003	0.0139	0.0657
Time 02	0.0381	0.0422	0.0827	0.0003	0.0149	0.0675
Time 03	0.0381	0.0477	0.0820	0.0003	0.0155	0.0701
Time 04	0.0381	0.0477	0.0817	0.0002	0.0089	0.0457
Time 05	0.0381	0.0477	0.0816	0.0002	0.0094	0.0470
Time 06	0.0381	0.0477	0.0816	0.0003	0.0141	0.0712
Time 07	0.0381	0.0477	0.0815	0.0005	0.0234	0.1035
Time 08	0.0381	0.0477	0.0815	0.0004	0.0199	0.0922
Time 09	0.0381	0.0477	0.0815	0.0003	0.0153	0.0723
Time 10	0.0381	0.0477	0.0815	0.0005	0.0214	0.0802
Time 11	0.0381	0.0477	0.0815	0.0005	0.0224	0.0838
Time 12	0.0381	0.0477	0.0815	0.0003	0.0164	0.0728
Time 13	0.0381	0.0477	0.0815	0.0004	0.0177	0.0764
Time 14	0.0381	0.0477	0.0815	0.0003	0.0157	0.0740
Time 15	0.0381	0.0477	0.0815	0.0003	0.0164	0.0758
Time 16	0.0381	0.0477	0.0815	0.0003	0.0135	0.0744
Time 17	0.0381	0.0477	0.0815	0.0003	0.0137	0.0655
Time 18	0.0381	0.0477	0.0815	0.0003	0.0133	0.0660
Time 19	0.0381	0.0477	0.0815	0.0002	0.0093	0.0493
Time 20	0.0381	0.0477	0.0816	0.0001	0.0079	0.0424
Time 21	0.0381	0.0477	0.0816	0.0019	0.0099	0.0509
Time 22	0.0381	0.0477	0.0817	0.0002	0.0084	0.0443

According to Table 3, one can opt for purely spatial modelling because, on average, this type of modelling has the smallest error. However, it is necessary to consider that the space-time model of Gneiting (2002) takes into account both the existing spatial dependence and temporal dependence, in addition to the possibility of making predictions for unsampled times. Table 1 shows that choosing the model of Gneiting (2002) does not result in much loss of information in the process of predicting values, which is the goal of geostatistics.

The space-time model is extremely useful for predicting unsampled values and is advantageous for obtaining missing data in the case of sensor failures or even cloud cover, showing a low magnitude of prediction error. The interpolation of unknown values is associated with the prediction, whereas the forescast is associated with the extrapolation of unknown values, so with the model proposed by Gneiting (2002), it is possible to forecast and predict these temperature values as a tool to concomitantly monitor the behaviour of phenomena over time and space. However, because this model is complex and requires software with the capacity to store and process complex and intense calculations, its use must be analysed, and resources for this processing should be obtained.

For the cases of the pure spatial analysis of phenomena, a separate spatial model for each time is justified by the fact this type of model yields a smaller prediction error and requires a simpler processing than the space-time model.

Most studies found in the literature for temperature spatialization used multiple linear regression (Medeiros et al., 2005; Bardin et al., 2010; Castro et al., 2010; Lyra et al., 2011, Gomes et al., 2014), which is a low-accuracy model for estimating values, showing the potential of both the purely spatial model and the space-time model for the spatialization of climatic elements, where the former has lower error and the latter has forecasting and prediction abilities.

CONCLUSIONS

It was possible to compare the space-time analysis with the purely spatial analysis using temperature data obtained by remote sensing images. The data modelled with the purely spatial analysis had, on average, lower error than those with the space-time model.

ACKNOWLEDGEMENTS. The authors thank, the Foundation for Research of the State of Minas Gerais (FAPEMIG), the National Council for Scientific and Technological Development (CNPq), the Coordination for the Improvement of Higher Education Personnel (CAPES), the Federal University of Lavras (UFLA) and University of Firenze (UniFI).

REFERENCES

Bardin, L., Pedro Júnior, M.J. & De Moraes, J.F. 2010. Estimation of maximum and minimum air temperatures for the 'Circuito das Frutas' region (São Paulo State, Brazil). *Revista Brasileira de Engenharia Agrícola e Ambiental* **14**(6), 618–624 (in Portuguese).

Bicalho, B.C. 2008. *Space-Time Models: Case Studies*. Masters dissertation, Federal University of Minas Gerais, Belo Horizonte, Brazil, 176 pp.

Cargnelutti Filho, A., Maluf, J.R.T. & Matzenauer, R. 2008. Geographic coordinates in the ten-day maximum and mean air temperature estimation in the State of Rio Grande do Sul, Brazil. *Ciência Rural* **38**(9), 2448–2456 (in Portuguese).

Castro, F.D.S., Pezzopane, J.R., Cecílio, R.A. & Pezzopane, J.E. 2010. Use of radar images to estimate air temperature. *Idesia* **28**(3), 69–79 (in Portuguese).

Cemek, B., Kucuktopcu, E. & Demir, Y. 2016. Determination of spatial distribution of ammonia levels in broiler houses. *Agronomy Research* **14**(2), 359–366.

Coelho, D.T., Sediyama, G. & Vieira, M. 1973. Estimates of average monthly and annual temperatures in the state of Minas Gerais. *Revista Ceres* **20**(112), 455–459 (in Portuguese).

Curi, T.M.R. de C., Vercellino, R. do A., Massari, J.M., Souza, Z.M. & Moura, D.J. de. 2014. Geostatistic to evaluate the environmental control in different ventilation systems in broiler houses. *Engenharia Agrícola* **34**(6), 1062–1074 (in Portuguese).

Dalanesi, P.E., Oliveira-Filho, A.T. & Fontes, M.A.L. 2004. Flora and structure of the arboreal component of the forest of the Parque Ecológico Quedas do Rio Bonito, Lavras, Minas Gerais State, and correlations between species distribution and environmental variables. *Acta Botanica Brasilica* **18**(4), 737–757 (in Portuguese).

Damasceno, F.A., Oliveira, C.E.A., Ferraz, G.A.S., Nascimento, J.A.C., Barbari, M. & Ferraz, P.F.P. 2019. Spatial distribution of thermal variables, acoustics and lighting in compost dairy barn with climate control system. *Agronomy Research* **17**(2), 385–395. https://doi.org/10.15159/ar.19.115

Dantas, A.A.A., Carvalho, L.G. & Ferreira, E. 2007. Climatic classification and tendencies in Lavras region, MG. *Ciência e Agrotecnologia* **31**(6), 1862–1866 (in Portuguese).

Fensholt, R., Sandholt, I., Stisen, S. & Tucker, C. 2006. Analysing NDVI for the African continent using the geostationary meteosat second generation SEVIRI sensor. *Remote Sensing of Environment* **101**(2), 212–229.

Ferraz, P.F., Yanagi Junior, T., Ferraz, G.A., Schiassi, L. & Campos, A.T. 2016. Spatial variability of enthalpy in broiler house during the heating phase. *Revista Brasileira de Engenharia Agrícola e Ambiental* **20**(6), 570–575.

Ferraz, P.F.P., Ferraz, G.A.S., Schiassi, L., Nogueira, V.H.B., Barbari, M. & Damasceno, F.A. 2019. Spatial variability of litter temperature, relative air humidity and skin temperature of chicks in a commercial broiler house. *Agronomy Research* **17**(2), 408–417. https://doi.org/10.15159/ar.19.112

Geiger, B., Carrer, D., Franchisteguy, L., Roujean, J.L. & Meurey, C. 2008. Land surface albedo derived on a daily basis from Meteosat second generation observations. *IEEE Transactions on Geoscience and Remote Sensing* **46**(11), 3841–3856.

Gneiting, T. 2002. Nonseparable, stationary covariance functions for space-time data. *Journal of the American Statistical Association* **97**(458), 590–600.

Gomes, D.P., Carvalho, D.F., de Oliveira Neto, D.H. & dos Santos, C.A. B. 2014. Estimated air temperature and reference evapotranspiration in the state of Rio de Janeiro. *Irriga* **19**(2), 302–314 (in Portuguese).

Hartkamp, A.D., De Beurs, K., Stein, A. & White, J.W. 1999. *Interpolation techniques for climate variables.* NRG-GIS Series 99-01. Mexico, D.F.: CIMMYT.

Honkavaara, E., Saari, H., Kaivosoja, J., Pölönen, I., Hakala, T., Litkey, P., Mäkynen, J. & Pesonen, L. 2013. Processing and assessment of spectrometric, stereoscopic imagery collected using a lightweight UAV spectral camera for precision agriculture. *Remote Sensing* **5**(10), 5006–5039.

Ligges, U., Maechler, M. & Schnackenberg, S. 2020. Scatterplot3d: 3D Scatter Plot R package version 0.3–41, URL https://cran.r-project.org/web/packages/scatterplot3d/scatterplot3d.pdf Acessed 23 april 2020

Lyra, G.B., Santos, M.J.D., Souza, J.L.D., Lyra, G.B. & Santos, M.A.D. 2011. Mapping annual air temperature in alagoas state, brazil, with different digital elevation models and spatial resolutions. *Ciência Florestal* **21**(2), 275–287 (in Portuguese).

Medeiros, R.M., Francisco, P.R.M., Santos, D., da Silva, L.L., Bandeira, M.M. & AESA, C.G.P. 2015. Variability of the Temperature Range of Air in the Paraíba State-Brazi. *Revista Brasileira de Geografia Física* **8**(01), 128–135 (in Portuguese).

Medeiros, S.S., Cecílio, R.A., Melo Junior, J.C.F. & Silva Junior, J.L. C. 2005. Estimation and spatialization of minimum, mean and maximum air temperatures for the Northeast region of Brazil. *Revista Brasileira de Engenharia Agrícola e Ambiental* **9**(2), 247–255 (in Portuguese).

Nychka, D., Furrer, R., Paige, J. & Sain, S. 2020. Fields: Tools for Spatial Data. R package version 9.6, URL https://cran.r-project.org/web/packages/fields/fields.pdf. Acessed 23 april 2020

Oliveira, C.E.A., Damasceno, F.A., Ferraz, P.F.P., Nascimento, J.A.C., Ferraz, G.A.S. & Barbari, M. 2019. Geostatistics applied to evaluation of thermal conditions and noise in compost dairy barns with different ventilation systems. *Agronomy Research* **17**(3), 783–796.

Padoan, S. & Bevilacqua, M. 2020. CompRandFld: Composite-Likelihood Based Analysis of Random Fields. R package version 1.0.3–5, URL https://cran.r-project.org/web/packages/CompRandFld/CompRandFld.pdf. Acessed 23 april 2020.

Pereira, I.M., Berg, E.V.D., Pinto, L.V.A., Higuchi, P. & Carvalho, D.A. 2010. Evaluation and proposal of connectivity of remnant fragments in the campus of Universidade Federal de Lavras, Minas Gerais. *Cerne* **16**(3), p. 305–321 (in Portuguese).

Pessanha, M.S., dos Santos, L.M., Lyra, G.B., Lima, A.O., Lyra, G.B. & de Souza, J.L. 2020. Interpolation methods applied to the spatialisation of monthly solar irradiation in a region of complex terrain in the state of Rio de Janeiro in the southeast of Brazil. *Modeling Earth Systems and Environment*, [online], p. 1–14. https://doi.org/10.1007/s40808-020-00878-8

R Core Team. 2020. R: A Language and Environment for Statistical Computing. Vienna, Austria. Disponível em: <https://www.R-project.org/>.

Ribeiro Júnior, P.J. & Diggle, P.J. 2020. GeoR: analysis of geostatistical data.R package version 1.7–5.2.1 URL https://cran.r-project.org/web/packages/geoR/geoR.pdf. Acessed 23 april 2020

Rodrigues, J.D.P., Alves, M.C., Freitas, A.S., Pozza, E.A., Oliveira, M.S. & Alves, H.J.P. 2019. Geostatistical stationary space-time covariance functions modeling of Yellow Sigatoka progress in banana crop. *Australasian Plant Pathology* **48**(3), 233–244.

Santos, L.M.D., Ferraz, G.A.S., Batista, M.L., Martins, F.B.S. & Barbosa, B.D.S. 2020. Characterization of noise emitted by a low-profile tractor and its influence on the health of rural workers. *Anais da Academia Brasileira de Ciência* [online], **92**(3). https://doi.org/10.1590/0001-3765202020200460

Schmetz, J., Pili, P., Tjemkes, S., Just, D., Kerkmann, J., Rota, S. & Ratier, A. 2002. An Introduction to Meteosat Second Generation (MSG). *Bulletin of the American Meteorological Society* **83**(7), 977–992.

Sherman, M. *Spatial Statistics and Spatio-Temporal Data: Covariance Functions and Directional Properties*. [S.l.]: Library of Congress Cataloging, 2011

Souza, J.S., Espirito-Santo, F.D.B, Fontes, M.A.L., Oliveira-Filho, A.T. & Botezelli, L. 2003. Analysis of the floristic and structural variations of a tree community in a tropical semideciduous forest fragment on the margins of the Capivari river, Lavras, southeastern Brazil. *Revista Árvore* **27**(2), pp. 185–206 (in Portuguese).

Varejão-Silva, M.A. 2006.*Meteorology and Climatology*. Recife: INMET.

Viana, R.S.M., dos Santos, G.R., Moreira, D.S., Louzada, J.M. & Rosa, L.M.F. 2019. The Use of Space-Temporal Geostatistics in the Prediction of Maximum Air Temperature. *Revista Brasileira de Geografia Física* **12**(1), pp. 096–111 (in Portuguese).